Unstable Chloronitrile Oxide, ClCNO, and Its Stable Ring Dimer: Generation, Spectroscopy, and Structure

Tibor Pasinszki*

Department of Inorganic Chemistry, Technical University of Budapest, H-1521 Budapest, Gellért tér 4, Hungary

Nicholas P. C. Westwood*

Guelph-Waterloo Centre for Graduate Work in Chemistry, Department of Chemistry and Biochemistry, University of Guelph, Guelph, Ontario, Canada N1G 2W1

Received: February 24, 1998; In Final Form: April 16, 1998

The unstable chloronitrile oxide molecule ClCNO has been generated from dichloroformaldoxime $Cl_2C{=}NOH$ by low-pressure gas-phase thermolysis or by a gas−solid reaction with HgO or metals. ClCNO is characterized in the gas phase by mid-infrared and HeI photoelectron spectroscopy, with the ground-state geometry obtained from ab initio calculations at the B3-LYP, MP*n* ($n = 2-4$), QCISD, QCISD(T), CCSD, and CCSD(T) levels using basis sets ranging from 6-31G** through 6-311G(2d) to cc-pVTZ. The calculated structure is strongly dependent upon the method employed and on basis set size, but is predicted to be linear or quasi-linear. The stable ring dimer, dichlorofuroxan, separately synthesized, does not yield the monomer upon thermolysis but leads to ClC(O)CN as a major product. The ring dimer has been investigated in the gas phase by infrared, photoelectron, and photoionization mass spectroscopy and also by ab initio calculations at the B3-LYP/6-31G** level. The same level of theory was applied to an investigation of the mechanism by which ClCNO dimerizes, this being found to be a typical two-step process; the first being formation of the C−C bond and the second the formation of the N−O bond with ring closure.

Introduction

The unstable chloronitrile oxide molecule ClCNO **1** was first generated as a transient species, unknowingly as it turns out,[1] by Kekulé in 1857[2] when he reacted mercuric fulminate with chlorine gas. The first direct detection of **1**, however, was made more than a century later by Maier and Teles using matrix infrared (IR) spectroscopy when dichloroformaldoxime, $Cl_2C{=}NOH$, was pyrolyzed in the gas phase at 600 °C and the products co-condensed with argon on a cold (10 K) window.[3] This remains the only physical measurement on **1** so far, with little known about its spectroscopy, structure, and stability in the dilute gas phase. **1** is very reactive, rapidly dimerizing to its stable furoxan dimer **2** (3,4-dichloro-1,2,5-oxadiazole 2-oxide), thereby precluding its isolation in the pure state. Nonetheless, it is widely used in organic synthesis, generated in situ from $Cl_2C{=}NOH$, and utilized for 1,3-dipolar cycloadditions.[4,5]

The four-atom **1** is spectroscopically and theoretically interesting due to its small size and potentially quasi-linear behavior. Early semiempirical MNDO[6] and ab initio Hartree−Fock (HF) calculations using a minimal STO-3G basis set[7] predicted a linear structure. Our recent ab initio calculations on BrCNO[8] and ONCCNO[9] and those on the parent nitrile oxide, fulminic acid HCNO,[10−14] show that inclusion of electron correlation is of crucial importance in predicting equilibrium structures for such nitrile oxides. The calculations indicated a pronounced effect of triple substitutions on the linear−bent question and, in addition, basis set size and inclusion of core electrons in the correlation energy calculations were also shown to be important. These questions are addressed herein using larger basis sets and including higher levels of electron correlation. Also, to connect to calculations on the dimer, dichlorofuroxan **2**, we have employed density functional theory (DFT), shown recently to be of value in assessing questions of linearity in HCNO.[15]

Dichlorofuroxan **2** readily forms upon dimerization of **1**, but the mechanism (one-step concerted or multistep) is not known. The reverse reaction, cleavage of **2** to **1**, is also an open question. We have observed the smooth thermolytic cycloreversion of dicyano- and dimethylfuroxans to NCCNO[16] and CH_3CNO,[17] respectively, but pyrolysis of dibromofuroxan yields, principally, ONCCNO, BrC(O)CN, and Br_2 rather than BrCNO.[8] Thermal decomposition of furoxans is thus influenced strongly by the substituent and requires special attention.

Wieland[1] correctly explained that **2** formed via a nitrile oxide intermediate in Kekulé's early experiment.[2] Subsequently a more convenient synthesis was discovered,[18] eliminating the use of the dangerous mercuric fulminate. More recently **2** has been recognized as an important component of nematocidal and fungicidal compositions.[19] Apart from liquid-phase IR/UV[18] and conventional mass spectroscopic[20] studies of **2**, NMR studies of dibromo- and diiodofuroxan,[21,22] and a dipole moment study of dibromofuroxan,[23] dihalofuroxans have not been extensively pursued by other experimental or theoretical tools. We have recently investigated dibromo-[8,24] and dicyanofuroxan[25] in the gas phase by IR and photoelectron (PE) spectroscopy and in the solid phase by Raman spectroscopy and X-ray diffraction. Both molecules are planar five-membered rings with an exocyclic nitrile oxide group and show unusual molecular or crystal

* Authors for correspondence. E-mail: pasinszki@ch.bme.hu, westwood@chembio.uoguelph.ca.

S1089-5639(98)01262-6 CCC: $15.00
Published on Web 06/05/1998

structures: e.g., bond lengths of dicyanofuroxan lie outside the standard range obtained for other known furoxans[25] and dibromofuroxan forms chiral crystals.[24] In both cases, standard HF and MP2 calculations have difficulty, with DFT proving to be a more viable computational approach.

In this paper we report the first gas-phase generation, IR, and PE spectra of **1** and a detailed investigation of its ab initio equilibrium structure using a variety of methods. **2** is characterized for the first time in the gas phase by PE and IR spectroscopies, by photoionization mass spectroscopy (PIMS), and by quantum chemical calculations employing DFT. Of particular interest are the structures and spectroscopy of **1** and **2** and the nature of the dimerization of **1**.

Experimental Section

The specifics of the generation of ClCNO **1** from $Cl_2C{=}NOH$ are given below in the Results and Discussion section. $Cl_2C{=}NOH$(s) was synthesized from trichloronitromethane;[26] dichlorofuroxan(l) **2** was synthesized by nitration of dichloroglyoxime with concentrated nitric acid.[18] The vapors of these precursors were then subject to fast flow thermolysis en route into the PE, PIMS, or IR chamber or cell.

HeI PE spectra were recorded on a fast pumping spectrometer specifically designed to study reactive/unstable species; resolution was 45 meV during experiments. Spectra were calibrated with the known ionization potentials (IPs) of O_2 and N_2. The instrument, a modification of an earlier version,[27] can also mass analyze ions produced in the photoionization process. A quadrupole mass analyzer (Hiden Analytical, 320 amu) with its EI source removed is mounted directly above the photoionization point, ionization being provided by HeI (21.2 eV) or unfiltered $HL_{\alpha,\beta,\gamma}$ (10.2−12.7 eV) radiation. PE and single-wavelength PIMS spectra can be recorded within seconds of each other; thus it is assumed that for a given PE spectrum the subsequent PIMS is of the same material.

IR spectra (0.5 cm^{-1} resolution, 4000−400 cm^{-1}) were collected on a Nicolet 20SXC FTIR using a 20 cm single-pass gas cell with KBr windows. The effluent from the pyrolysis (for **1**) or sample container (for **2**) was pumped continuously through the cell using a rotary pump while maintaining the pressure between 350 and 400 mTorr (for **1**) and ca. 500 mTorr (for **2**).

Computational Methods

Ab initio calculations for **1** were carried out at the MP2, MP3, MP4, QCISD, QCISD(T), CCSD, and CCSD(T) levels using standard basis sets: 6-31G**, 6-311G(2d), or cc-pVTZ (Dunning's correlation consistent basis set, [5s, 4p, 2d, 1f] on Cl and [4s, 3p, 2d, 1f] on C, N, and O). DFT was also used to calculate equilibrium structures for **1** in the form of Becke's three-parameter exchange functional in combination with the Lee, Yang, and Parr (LYP) correlation functional (B3-LYP). The structure of **2** was calculated using the B3-LYP method and a 6-31G** basis set. Equilibrium molecular geometries were fully optimized and harmonic vibrational frequencies were then calculated using numeric second derivatives to confirm real minima on the potential energy surface (zero imaginary frequency). Transition states (first-order saddle points) and second-order saddle points were characterized with one or two imaginary frequencies, respectively. IPs for **1** and **2** were calculated using Koopmans' theorem (KT)[28] and the Outer Valence Green's Function (OVGF) method.[29] In the OVGF calculation for **1**, all electrons were included in the correlation calculation, whereas for **2** the 22 occupied valence shell molecular orbitals (MOs) and the 12 lowest lying unoccupied MOs were included. All calculations were performed with the Gaussian-92 and Gaussian-94 quantum chemistry packages[30,31] implemented on a Silicon Graphics Inc. Challenge/XL workstation.

SCHEME 1

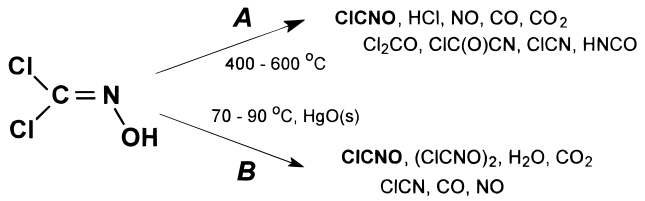

Results and Discussion

Chloronitrile Oxide, 1. *Generation and Identification.* Two routes to ClCNO **1** were considered: the thermolysis or base treatment of $Cl_2C{=}NOH$ or the thermolysis of the stable dimer **2**. All of the following observations were confirmed by PE, PIMS, and IR measurements.

Thermolysis of $Cl_2C{=}NOH$ was carried out in a quartz tube (8 mm i.d.) heated along 15 cm; for a more efficient pyrolysis, the tube was loosely packed with quartz chips. Formation of **1** and HCl (the desired elimination product) commenced at 400 °C, but at this temperature large amounts of precursor emerged unchanged from the furnace. Increasing temperature decreased the amount of unreacted precursor, but at the expense of increasing amounts of side products such as NO, CO, CO_2, $Cl_2C{=}O$, ClC(O)CN, ClCN, and HNCO (Scheme 1, path A).

Destruction of $Cl_2C{=}NOH$ was complete at 600 °C, but at this temperature **1** was only a minor component. Increases to 700 °C led to a complete absence of the ν_{as}/ν_s(CNO) IR bands of **1**, which, it should be pointed out, have a large oscillator strength and are distinctive for nitrile oxides.[32] The **1**/HCl ratio determined from the IR intensities gradually decreased with increasing temperature, indicating that **1** was not thermally stable at higher temperature.

To achieve higher conversion to **1** at lower temperatures, metal chips (Cu, Al, Fe) were used instead of quartz, although $Cl_2C{=}NOH$ reacted with the metals above 400−500 °C forming, among other products, HNCO which overlaps with ν_{as}(CNO). With Al metal, formation of the isocyanate isomer, ClNCO, of **1** was observed. The best conversion of $Cl_2C{=}NOH$ to **1** was obtained using Cu chips at 400 °C. Figure 1a shows the raw IR spectrum of this reaction, illustrating the presence of the distinctive ν_{as}(CNO) and ν_s(CNO) bands at ca. 2220 and 1340 cm^{-1}, respectively, together with the presence of HNCO, ClC(O)CN, and some unreacted precursor bands (ν_4/ν_5 at ca. 1000 cm^{-1}).[33] ClCN is present also, although the CN stretch (2219 cm^{-1})[34] with a low oscillator strength does not intrude on the structure around 2250 cm^{-1}.

We have previously noted[8] that gaseous $Br_2C{=}NOH$ rapidly reacts at room temperature with solid HgO or gaseous NH_3 forming BrCNO. These reactions were attempted with $Cl_2C{=}NOH$, but to no avail. A rapid reaction does occur, however, between $Cl_2C{=}NOH$(g) and HgO(s) at slightly elevated temperatures, 70−90 °C (Scheme 1, path B). Figure 1b shows the raw IR of this reaction, more clearly evincing ν_{as}(CNO). In addition to **1**, the stable dimer **2** (band at ca. 1650 cm^{-1}), H_2O, CO_2, ClCN (hidden under ν_{as}(CNO)), CO, and NO were identified among the reaction products.

Given that **2** readily forms upon dimerization of the monomer **1**, a potential route to **1** is the thermal cycloreversion of **2**. For

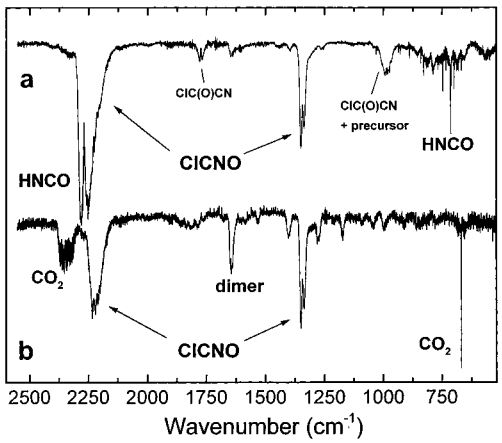

Figure 1. (a) Mid-IR spectra of the thermolysis of $Cl_2C{=}NOH$ over Cu chips at 400 °C and (b) mid-IR spectra of the flow reaction of $Cl_2C{=}NOH$(g) with HgO(s) at 70 °C. In both spectra ClCNO **1** is identified, along with other species.

SCHEME 2

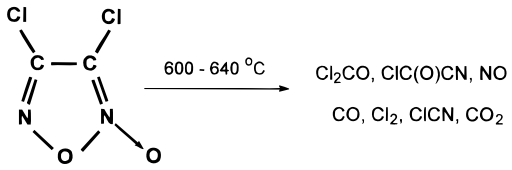

the high-yield generation of NCCNO[16] and CH_3CNO[17] from their stable dimers, this is the method of choice. Formation of **1**, however, was not found upon pyrolysis of **2** over quartz chips (Scheme 2). The major products from this reaction at 600−640 °C are $Cl_2C{=}O$ and ClC(O)CN, with NO, CO, Cl_2, ClCN, and CO_2 as side products.

We note here that ClC(O)CN (cyanoformyl chloride) has previously been obtained by thermolysis of ClC(O)CClNSCl at 800 °C,[35] although its spectroscopy and structure are unknown. The use of **2** (and its bromo analog) as precursor to ClC(O)CN (and the unknown BrC(O)CN) turns out to be a novel method for examining their spectroscopy.[36]

Infrared Spectrum of ClCNO. As noted above, and illustrated in Figure 1, a clean route to **1** was not achieved. Nevertheless, three IR bands of **1** were unambiguously observed, confirming the gas-phase identity of this molecule and concurring with the earlier Ar matrix work.[3] Experimental and calculated vibrational frequencies, calculated IR intensities, and band assignments are shown in Table 1.

The five fundamentals, assuming linearity, comprise three stretching modes of σ symmetry and two bending modes of π symmetry, all IR active. Down to 400 cm^{-1}, only the two strongest fundamentals (see Table 1 for calculated intensities) are observed, the antisymmetric (ν_1) and symmetric (ν_2) CNO stretches at 2219 and 1343 cm^{-1}, together with the first overtone of ν_2 at 2688 cm^{-1}. The Cl−C stretching (ν_3) and CNO bending (ν_4) modes are weak (Table 1) and, although calculated above 400 cm^{-1}, are not observed. The ClCN bend (ν_5) is likely well below 100 cm^{-1}. The three observed bands correlate to those of BrCNO at 2632, 2211, and 1321 cm^{-1} [8,37] and show very similar band profiles. The symmetric CNO stretch at 1343 cm^{-1} with a PR separation of ca. 14 cm^{-1} shows the typical parallel band structure associated with a linear molecule. The ν_1(CNO) band at 2219 cm^{-1} displays rather complicated structure similar to that of BrCNO[8] and ONCCNO[9] arising from hot bands of the lowest bending vibration.

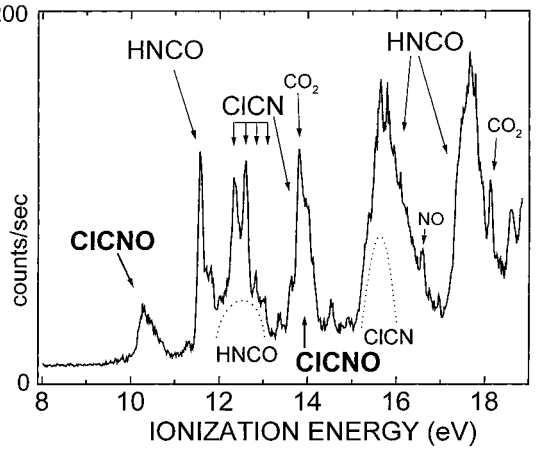

Figure 2. HeI photoelectron spectrum of the thermolysis of $Cl_2C{=}NOH$ over Cu chips at 400 °C. Reaction products are identified

The calculated positions of ν_1 and ν_2 are in reasonable agreement with experiment given that they are unscaled harmonic frequencies. The calculations for the structure (below) provide evidence for a quasi-linear structure, as do the exceptionally low frequencies of 16 cm^{-1} (B3-LYP/cc-pVTZ) and 32 cm^{-1} (QCISD/6-311G(2d)) calculated for the lowest energy bending motions (Table 1). The frequency of the lowest bending mode in NCCNO, a molecule regarded as being more "linear" than ClCNO (and BrCNO) is estimated at 86 cm^{-1} from an analysis of combination bands in the high-resolution IR spectrum.[38]

HeI Photoelectron Spectrum of ClCNO. Figure 2 shows the raw PE spectrum of the thermolysis of $Cl_2C{=}NOH$ over Cu chips at 400 °C. The conditions are thus similar to those of the IR (Figure 1a) and demonstrate the complementarity of the IR and PE results. Marked are strong bands of HNCO[39] and ClCN,[40] the latter barely showing in the IR. Traces of CO_2

TABLE 1: Experimental[a] and Calculated[b] Vibrational Frequencies (cm^{-1}) of ClCNO

experimental		calculated				
		B3-LYP/cc-pVTZ		QCISD/6-311G(2d)		
gas	matrix[c]	freq	int[d]	freq	int[d]	assignment and description
2688	2643.5					$2\nu_2$
2219	2281.4[e] 2261.7[e]	2456 (σ)	330.2	2458 (σ)	312.1	ν_1 CNO as str
1350 R 1336 P	1326.3	1373 (σ)	315.9	1330 (σ)	273.6	ν_2 CNO sym str
		626 (σ)	0.1	613 (σ)	0.6	ν_3 Cl−C str
		466 (π)	5.5	470 (π)	5.9	ν_4 CNO bend
		16 (π)	0.1	32 (π)	0.0	ν_5 ClCN bend

[a] Band positions (gas) taken from the maxima of the IR bands. [b] Unscaled harmonic frequencies. [c] Reference 3. [d] In km/mol. [e] Splitting due to matrix effects.

TABLE 2: Experimental and Calculated Ionization Potentials (eV) of ClCNO and BrCNO

ClCNO		BrCNO			
expt IP[b]	calc[a] OVGF	expt IP[b]	calc[a] OVGF	ionic state	orb. character
10.28	9.92	10.05	9.72	$\tilde{X}^2\Pi$	π_{nb}(CNO)
(13.8)[c]	13.87	12.91	12.92	$\tilde{A}^2\Pi$	$\pi(n_x)$
n.o.[d]	16.68	15.80	16.42	$\tilde{B}^2\Pi$	π_b(CNO)
n.o.[d]	17.83	17.14	17.14	$\tilde{C}^2\Sigma$	$\sigma(n_o)$

[a] The B3-LYP/6-31G** geometry was used. [b] Vertical ionization potentials. [c] Partly under ClCN and CO_2 bands. [d] Not observed.

and NO are also observed. In addition, two new bands appear at 10.28 and 13.8 eV, the latter partially masked by the known structure of the $\tilde{A}^2\Sigma$ state of $ClCN^+$ at 13.80 eV and the coincident sharp peak of CO_2^+ at 13.80 eV.[41] The PIMS recorded at the same time as the PES shows strong parent ion ($ClCNO^+$) and fragment NO^+ mass peaks consistent with the PIMS of other nitrile oxides[8,9,16,17] and only the merest trace of precursor. Given this, and the evidence of the IR spectrum under identical conditions, the two new bands are assigned to the $\tilde{X}^2\Pi$ and $\tilde{A}^2\Pi$ states of $ClCNO^+$. Table 2 shows these data, together with the four OVGF calculated IPs expected in the HeI region. Also given are the corresponding experimental and OVGF IPs for the related BrCNO molecule for which the experimental data is much more clear. The data clearly demonstrates that the two observed bands belong to ClCNO, both from their positions compared to BrCNO and from the trends in the OVGF calculations. The $\tilde{B}^2\Pi$ and $\tilde{C}^2\Sigma$ states of $ClCNO^+$ lie hidden under the intense HNCO bands at 16 and 17.5 eV.

Calculated Structure of ClCNO. From previous experimental and theoretical work on substituted nitrile oxides, XCNO (X = H,[42] Br,[8,37] NC,[16,38,43] ONC[9,44]) it is clear that **1** is likely to have a linear or quasi-linear structure. The parallel band structure of ν_2 suggests this, but lacking other experimental evidence, quantum chemical calculations can provide an assessment of the structure. In previous work on BrCNO,[8] computational resources hampered our ability to examine thoroughly this question, although it is clear that such molecules present interesting challenges for ab initio methods. For the linear/bent question there are strong basis set and correlation level dependencies for equilibrium structures, including effects of including core electrons, triple substitutions, and the efficacy (or otherwise) of using DFT methods. Given that **1** is computationally more viable than BrCNO, we now present a computational strategy for the structure and barrier to linearity that illustrates many of the subtle influences extant in this kind of molecule.

First the geometry of **1** was computed using levels of theory from HF through MP*n* to QCI and CC with a 6-31G** basis set, excluding core electrons from the correlation energy calculations (fc, "frozen-core"). This was repeated with a larger basis set, 6-311G**. Then core electrons were included ("full") for these two basis sets, and finally the basis set size was increased to cc-pVTZ where resources allowed. The results are illustrated in Table 3. The given structures refer to the largest basis set feasible at a given level of electron correlation.

As shown by the calculated barrier to linearity, only HF (not given in Table 3) and MP3 calculations at the smallest basis set (fc/6-31G**) predict a linear structure for **1**, while other MP*n*, QCI, and CC calculations with the same basis set gave bent structures but with significant differences in the ClCN angle and barrier to linearity. Both increasing the basis set size (6-31G** → 6-311G(2d) → cc-pVTZ), and including core electrons in the correlation energy calculations lead to a diminution in the calculated barrier height. With "full" and the biggest feasible basis sets, the molecule is predicted to be linear using B3-LYP, MP3, MP4SDQ, QCISD, and CCSD. Resource limitations precluded further increases in basis set size at the MP4SDTQ, QCISD(T), and CCSD(T) levels, but the trend indicates further decreases in the barrier for higher levels of theory. This would be in keeping with recent large scale ab initio calculations[14] on HCNO using the CCSD(T) method, where the barrier decreased from 261 → 42 → 7 cm^{-1} using the basis sets cc-pVDZ through cc-pVTZ to cc-pVQZ, respectively.

The variation in the calculations demonstrates an unusually strong effect of triple excitations on the barrier height and geometry, with triples markedly increasing the barrier height and decreasing the ClCN angle (compare MP4SDQ vs

TABLE 3: Calculated Barrier to Linearity, Equilibrium Structure, Total Energies, Rotational Constants, and Dipole Moment of ClCNO[a]

	B3-LYP	MP2	MP3	MP4SDQ	MP4SDTQ	QCISD	QCISD(T)	CCSD	CCSD(T)
					Barrier to Linearity				
basis set									
fc/6-31G**	37	784	0	263	1266	195	628	96	582
full/6-31G**	37	676	0	184	1132	125	514	43	470
fc/6-311G(2d)	4	543	0	57	991				
full/6-311G(2d)	4	445	0	6	864	0	296	0	
full/cc-pVTZ	0	299	0	0					
					Structure for the Largest Basis Set				
Cl−C	1.637	1.643	1.634	1.639	1.682	1.654	1.677	1.654	1.668
C−N	1.157	1.189	1.145	1.154	1.205	1.155	1.185	1.153	1.191
N−O	1.205	1.191	1.197	1.205	1.211	1.216	1.208	1.212	1.218
ClCN	180.0	151.8	180.0	180.0	144.7	180.0	146.9	180.0	147.2
CNO	180.0	170.5	180.0	180.0	166.5	180.0	169.7	180.0	169.5
tot. energy	−628.25467	−627.47230	−627.46001	−627.47257	−627.46008	−627.40596	−627.44355	−627.40193	−627.17560
A[b]		336.266			221.379		232.534		240.061
B	2.508	2.593	2.536	2.508	2.564	2.477	2.582	2.484	2.573
C		2.573			2.535		2.554		2.545
μ[c]	3.08	3.34	3.87	4.24	3.08	4.07	3.19	4.17	3.36

[a] Barrier to linearity in cm^{-1}, bond angles in deg, bond lengths in Å, total energies in a.u. The given structures are at the largest basis set: viz., cc-pVTZ at the B3-LYP, MP2, MP3, and MP4SDQ levels; 6-311G(2d) at the MP4SDTQ, QCISD, QCISD(T), and CCSD levels; 6-31G** at the CCSD(T) level; all electrons were included in the correlation energy calculations ("full"). [b] Rotational constants in GHz. Isotopes: Cl-35, C-12, N-14, O-16. [c] Dipole moment in Debye.

MP4SDTQ, QCISD vs QCISD(T), and CCSD vs CCSD(T)). By including a better description of triple excitations, both T correlation effects and TT coupling, in the order MP4SDTQ → QCISD(T) → CCSD(T), the calculated barrier height decreases. Tracking the MP*n* expansion series (MP1 = HF, MP2, MP3, MP4) using the 6-311G(2d) basis set, an oscillatory behavior can be seen not only in the calculated barrier height (0, 445, 0, 864 cm^{-1}) but also the geometry (especially the ClCN angle and CN bond length) and the total energy. The possibility of oscillatory behavior of the MP*n* series is known;[45,46] starting from MP1, MP2 exaggerates the effects of the new incoming terms (the double excitations), MP3 underestimates these due to DD coupling, MP4 exaggerates the new triple effects (and strongly overestimates the barrier height), and MP5 underestimates these due to TT coupling.[46] The pronounced oscillations in the calculated parameters are a strong indication of large electron correlation effects and so their precise description is of crucial importance.

The level of theory employed determines not only the bond angles and barrier to linearity but also the bond lengths, especially the CN bond, which is correlated with the ClCN angle: the longer the CN bond the smaller the ClCN angle. The description of the CN bond length is probably the most critical in this molecule, and since the inclusion of triple effects reduces the ClCN angle, the CN bond lengthens. Increasing the basis set size and including a better description of triple effects in the series, MP4SDTQ → QCISD(T) → CCSD(T) then decreases the CN bond length.

The conclusion is that the calculated equilibrium geometry of **1** changes markedly depending upon the level of theory, but that there are clear trends in bond lengths, angles, and barrier height as a function of the method employed, basis set size, and the effect of core electrons and triple substitutions. Clearly **1**, and nitrile oxides in general, present interesting computational challenges, but the evidence is that **1** must be a linear or quasi-linear molecule. To assist in future detection of **1** by high-resolution spectroscopy, Table 3 also includes the calculated rotational constants and dipole moments. We note here that ClCNO has been recently detected by millimeter wave spectroscopy,[47] with the determined rotational constants best matching those from the MP2/cc-pVTZ, QCISD(T)/6-311G(2d), and CCSD(T)/6-31G** levels of theory.

Dichlorofuroxan, 2. *Calculated Structure.* The structure of this molecule, the ring dimer of **1**, is unknown, as is its gas-phase spectroscopy. We have recently investigated the theoretical and experimental structures of dicyano-[25] and dibromofuroxan[24] using HF, MP2, and B3-LYP/6-31G**, and X-ray diffraction. A comparison of the calculated equilibrium structures and the experimental crystallographic data, where we expect differences to be small for such rigid species, indicates that both HF and MP2 methods perform poorly, failing to describe accurately the structures especially for the three interconnected N−O bonds. On the other hand, the structures and vibrational frequencies calculated by B3-LYP/6-31G** showed surprisingly good agreement with experiment. Given this and the fact that conventional ab initio methods are not cost-effective for the ring dimer **2**, we have chosen to use B3-LYP/6-31G** to calculate its properties.

The calculated structure is shown in Table 4 along with calculated Wiberg bond orders obtained from an NBO analysis.[48] The molecule is planar, the C−N bond lengths and bond orders implying imine-like partial double-bond character, and the C−C bond, nominally a single bond, is slightly shorter than a C−C single bond. The longest bond in the ring frame, with a small (0.9) bond order, is O_1-N_2, a possible point of cleavage, calculated to be 1.463 Å, close to the crystal structure values of 1.438 and 1.454 Å for dibromo-[24,32] and dicyanofuroxan,[25,32] respectively. The exocyclic N_2-O_6 bond is the shortest among the N−O bonds, with a bond order of 1.5, indicating that the molecule cannot be simply described as a five-membered ring with an exocyclic nitrile oxide group. Another mesomeric structure, a five-membered ring with an exocyclic nitrosyl group, is also important in the description. A full description of the structure and charge distribution requires additional mesomeric structures and supports again the notion that the electron distribution in furoxans is unusual and cannot be described by just two or three simple mesomeric structures.[23]

TABLE 4: Calculated[a] Equilibrium Structure of Dichlorofuroxan

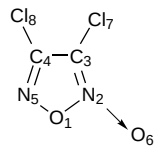

N_2-O_6	1.214 (1.5)	$O_1-N_2-C_3$	105.5
N_5-O_1	1.373 (1.1)	$N_2-C_3-C_4$	107.1
O_1-N_2	1.463 (0.9)	$C_3-C_4-N_5$	112.2
N_2-C_3	1.334 (1.3)	$C_4-N_5-O_1$	106.3
C_3-C_4	1.421 (1.2)	$N_5-O_1-N_2$	108.7
C_4-N_5	1.304 (1.6)	$C_3-N_2-O_6$	135.3
C_3-Cl_7	1.698 (1.1)	$C_4-C_3-Cl_7$	130.9
C_4-Cl_8	1.712 (1.1)	$C_3-C_4-Cl_8$	125.7

[a] Calculated at the B3-LYP/6-31G** level of theory. Bond lengths in Å and bond angles in deg. Total energy: −1256.377237 au. Calculated bond orders in parentheses.

The calculated charge on the furoxan moiety (−0.24 *e*, obtained from the Mulliken population analysis) is reduced compared to the parent furoxan (−0.31 *e*)[25] owing to the electron-withdrawing Cl substituents. There is a large negative charge (−0.41 *e*) on the exocyclic oxygen and a large positive charge (+0.32 *e*) on the connected nitrogen, which makes the exocyclic N_2-O_6 bond very polar. The endocyclic oxygen is also negative (−0.23 *e*) but less so than the exocyclic oxygen, and the negative charge on N_5 is even smaller (−0.12 *e*). There is little positive charge on the carbon atoms (+0.09 and +0.11 *e*) and surprisingly also on the Cl substituents (+0.11 and +0.13 *e*). Overall the calculated structure of the ring moiety is very close to that calculated for dibromofuroxan,[24,32] as are the calculated charges.

Photoionization Mass Spectra of 2. The HeI and $HL_{\alpha,\beta,\gamma}$ PIMS of **2** are shown in Figure 3 and can best be characterized as a single peak at mass 30 (NO^+), comparable to that observed in the conventional electron-impact (EI) mass spectrum of **2**[20] and in the PIMS study of dibromo-[8] and dicyanofuroxan.[25] This can be attributed to easy cleavage of the N−O and C−N bonds in furoxans. With higher detector sensitivity, the molecular ion at $m/z = 154$ (^{35}Cl) with the characteristic 9:6:1 pattern for two Cl atoms and other fragments can be observed with intensities some 2−3 orders smaller than those of NO^+. Ion fragments in the HeI PIMS (Figure 3a) derived from M^+ by losing one or two NO groups ($M-(NO)^+$, $M-(NO)_2^+$) and the fragment $(NO)_2^+$ have also been observed in mass spectra of substituted furoxans[8,20,25] and are characteristic of the furoxan group. Other fragments in the HeI PIMS at m/z = 47, 54, 63, 73, 89, 108 (^{35}Cl) correspond to ClC^+, C_2NO^+, ClN_2+, ClC_2N^+, ClC_2NO^+, $Cl_2C_2N^+$, respectively. Overall, the HeI PIMS and 70 eV EI mass spectra of **2** are very similar. The fragmentation is reduced in the $HL_{\alpha,\beta,\gamma}$ PIMS (Figure 3b), and together with the dominant

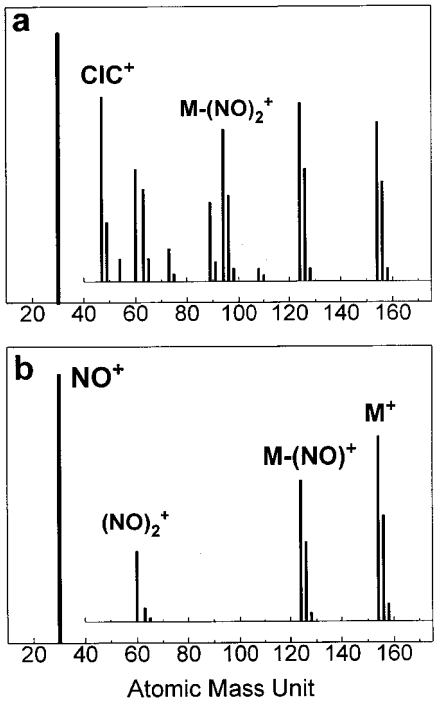

Figure 3. (a) HeI and (b) $HL_{\alpha,\beta,\gamma}$ photoionization mass spectra (amu) of dichlorofuroxan **2**. Note scale above 40 amu is enhanced by a factor of 10^3.

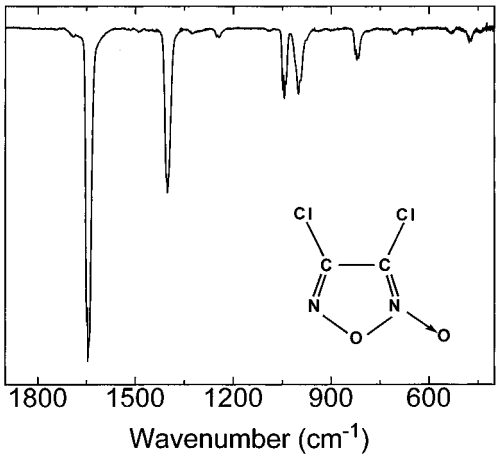

Figure 4. Mid-IR spectrum of dichlorofuroxan, **2**.

NO^+ peak, only the parent ion (M^+), $M-(NO)^+$, and $(NO)_2^+$ are observed. Although formation of the $M-(NO)_2^+$ ion is evident in both HeI PIMS and EI mass spectra of substituted furoxans, it is not observed in the $HL_{\alpha,\beta,\gamma}$ PIMS of any disubstituted furoxan we have studied[8,25] and may thus be regarded as typical of the $HL_{\alpha,\beta,\gamma}$ PIMS of furoxans.

Infrared Spectrum of ***2.*** The IR spectrum of gaseous **2** is shown in Figure 4 with calculated and experimental frequencies listed in Table 5. The IR of the liquid[18] has been noted before and is in general accord with the data given here. The calculated frequencies and IR intensities are in good agreement with experiment and support the band assignments. It has been concluded from IR investigations of several aryl-, acyl-, and alkylfuroxans in various solvents[49] that no absorption bands characteristic of the furoxan group appear between 4000 and 1800 cm^{-1}. We have found the same for dibromo-[8] and dicyanofuroxan,[25] with the same holding true for **2**. Since the bands which originate from the C−Cl in- and out-of-plane deformations are expected to be below 400 cm^{-1} and the IR intensity of C−Cl stretches are small (see calculated values in Table 5), all strong IR bands observed in the 1800−400 cm^{-1} region can be assigned to the furoxan ring. The most characteristic absorption, assigned to the C═N double bond, usually appears in the 1650−1600 cm^{-1} region. This absorption is observed at 1646 cm^{-1} in the spectrum of **2**. According to the calculations, this normal mode also possesses some N→O character, and may be described as the antisymmetric C═N→O stretch. Its symmetric counterpart gives rise to a small band at 1244 cm^{-1}. The IR band from the second C═N stretch is expected between 1600 and 1500 cm^{-1}, and most spectra of aryl-, acyl-, and alkylfuroxans[48] show this band, anywhere between weak and strong. This band, however, was not observed in the spectra of dibromo-[8] and dicyanofuroxan[25] and also is not seen in the case of **2**, in good agreement with the calculation which predicts a very low IR intensity. The next four bands at 1401, 1044, 1001, and 821 cm^{-1} can be unambiguously assigned to the furoxan group; they have been observed in the spectra of all furoxan derivatives investigated so far,[8,25,49] although an unambiguous assignment for all bands is not entirely possible due to the strong mixing of normal modes, arising from similar atomic masses within the furoxan group. There are five weak bands in the 750−400 cm^{-1} region from which, by analogy with the spectrum of the dibromo derivative,[8,24] the bands at 703, 651, and 474 cm^{-1} can be assigned to the furoxan group deformations. The remaining two bands at 531 and 441 cm^{-1} are assigned to the two C−Cl stretches.

TABLE 5: Experimental and Calculated Vibrational Frequencies (cm^{-1}) of Dichlorofuroxan

exptl IR[a]	calcd freq[b]	calcd intensity[c]	assignment and description
1646 vs	1732 (a′)	411.2	ν_1 ring str (C═N→O as. str)
n.o.[d]	1525 (a′)	2.5	ν_2 ring str (C═N)
1401 s	1417 (a′)	153.4	ν_3 ring str (C−C)
1244 vw	1278 (a′)	12.8	ν_4 ring str (C═N→O sym str)
1044 m	1063 (a′)	44.2	ν_5 ring vibr
1001 m	1018 (a′)	118.4	ν_6 ring vibr
821 w	832 (a′)	24.8	ν_7 ring vibr
703 vw	714 (a′)	6.1	ν_8 ring vibr
651 vw	657 (a″)	5.1	ν_{14} out-of-plane def
n.o.	569 (a″)	0.7	ν_{15} out-of-plane def
531 vw	525 (a′)	4.5	ν_9 C−Cl sym str
474 vw	485 (a′)	8.2	ν_{10} ring def
441 vw	441 (a′)	1.2	ν_{11} C−Cl as. str
n.o.	374 (a″)	0.4	ν_{16} out-of-plane def
n.o.	283 (a′)	1.4	ν_{12} C−Cl in-plane as. def
n.o.	254 (a″)	2.8	ν_{17} out-of-plane def
n.o.	162 (a′)	0.3	ν_{13} C−Cl in-plane sym. def
n.o.	132 (a″)	0.2	ν_{18} out-of-plane def

[a] Gas phase; additional very weak features at 1692, 1326 and 1090 cm^{-1}. [b] Unscaled harmonic frequencies; calculated at the B3-LYP/6-31G** level of theory. [c] IR intensities in km/mol. [d] Not observed

Photoelectron Spectrum of ***2.*** The HeI PE spectrum is shown in Figure 5 with experimental IPs listed in Table 6. KT[28] IPs and those from the OVGF[29] method were calculated using the B3-LYP/6-31G** structure and are also listed in Table 6. The KT deficiency of overestimating IPs, especially in the high IP region is well known, whereas the OVGF method gives very good agreement with experiment. From the calculated IPs and from a comparison with the known PE spectra of the dibromo and dicyano[8,25] derivatives, the assignment is relatively straightforward.

A starting point in describing the electronic structure of **2**, also applied to the dibromo-[8] and dicyanofuroxan[25] PE spectra, is to consider the molecular orbitals of a furazan ring,[50] modified with an exocyclic oxygen atom and mixed with MOs arising

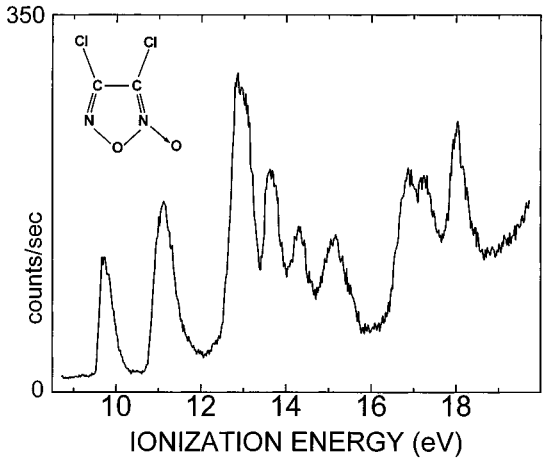

Figure 5. HeI photoelectron spectrum of dichlorofuroxan **2**.

TABLE 6: Experimental and Calculated Ionization Potentials (eV) of Dichlorofuroxan

	calcd[a]		
exptl IP[b]	HF/Koopmans	OVGF	orb. character
9.69	10.27 (a″)	9.27	π (n_O)
11.10	12.28 (a″)	10.84	π
	13.05 (a′)	11.25	σ (n_O)
12.84	14.05 (a′)	12.79	n_{Cl}
12.84	14.29 (a′)	12.89	n_{Cl}
13.10 (sh)	14.67 (a″)	13.26	n_{Cl}
13.65	15.97 (a″)	14.28	n_{Cl}
14.31	16.06 (a′)	13.75	σ (n_N)
15.15	17.14 (a′)	15.17	σ ($n_{O,\ ring\ oxygen}$)
	17.23 (a″)	14.68	π
16.90	18.45 (a′)	16.88	σ
17.26	19.45 (a′)	17.26	σ
18.04	20.66 (a′)		σ

[a] The B3-LYP/6-31G** geometry was used. [b] Vertical ionization potentials.

from the two Cl substituents. The first band in **2** at 9.69 eV originates from the exocyclic oxygen (O_6) out-of-plane lone pair $\pi(n_O)$ mixed with the high lying furazan ring π orbitals (11.8 eV in the parent furazan[50]). The second band at 11.10 eV is assigned to two MOs; one is the high lying furazan-like π MO mixed with some Cl character, and the other is the exocyclic O_6 in-plane $\sigma(n_O)$ lone pair mixed with the furazan ring σ framework orbitals. This concurs with the high lying (8−10 eV) O pπ and pσ orbitals separated by ca. 1 eV in relatively simple *N*-oxides, e.g., pyridine *N*-oxides,[51] and is a characteristic fingerprint for furoxans, being observed in the spectra of the dibromo-,[8] dicyano-,[25] and dimethylfuroxans.[17] Between 12 and 14 eV, the two bands, one centered at ca. 13 eV and the other at 13.65 eV, must accommodate the two in- and two out-of-plane Cl lone pair orbitals. The distribution, based on the relative intensities and the calculations, is such that three MOs are assigned to the 13 eV band and one to the band at 13.65 eV. Similar bands are observed in the spectra of 3,4-dichlorothiophene[52] (11.5−12.6 eV) and *cis*-1,2-dichloroethylene[41] (11.8−14.1) eV, which also indicate that the out-of-plane MOs shift toward higher energy. This is also observed in **2,** due to mixing with the ring π orbitals, with all n_{Cl} based orbitals shifted to higher energy compared to the other dichloro- analogs due to the electronegative N and O atoms in the furoxan group. The weaker band at 14.31 eV is then assigned to the higher lying furazan-like σ orbital, which is mainly localized on the ring N atom (calculated value by OVGF is 13.75 eV). The broad band at 15.15 eV, by analogy with the comparable band in dibromofuroxan[8] at 14.6 eV, can be assigned to two MOs: one, the next furazan-like σ orbital with a dominant contribution from O_1, and the other, the second furazan-like π MO. There are three other bands assigned to σ MOs between 16 and 19 eV. An unambiguous assignment is not possible due to the delocalization over the entire σ framework; calculations indicate that the MO corresponding to the band at 16.90 eV has some C−Cl character.

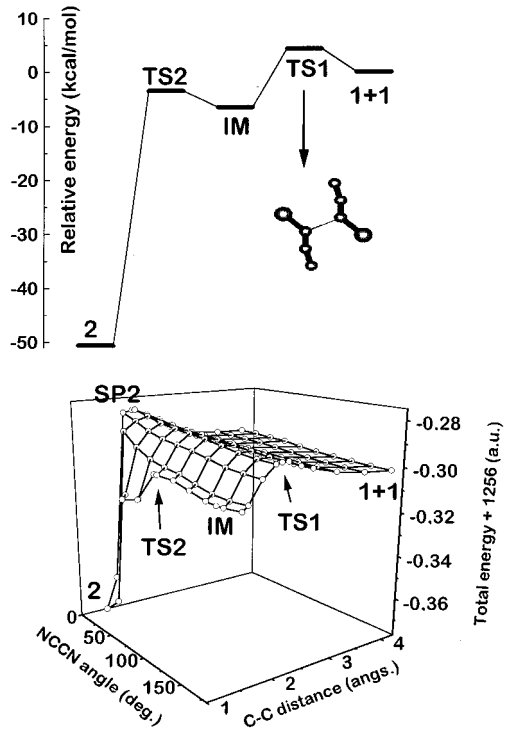

Figure 6. Potential surface for the dimerization of ClCNO, **1**, and relative energies of stationary points. See text for discussion.

Dimerization of Chloronitrile Oxide 1 to Dichlorofuroxan 2. 1,3-dipolar cycloadditions leading to five-membered heterocycles are the most important reactions of nitrile oxides and have great preparative importance. The first general mechanism for 1,3-dipolar cycloadditions was suggested by Huisgen[53,54] in the early sixties, a one-step, concerted, cycloaddition mechanism in which the two new σ bonds are formed simultaneously at the cost of two π bonds. This mechanism became widely accepted and was not questioned until the work of Firestone[55] in 1968 which proposed a two-step mechanism, in which only one σ bond forms in the first step, leading to an intermediate of either cyclo- or extended conformation. In a second step, this intermediate would close to the final five-membered ring after passing over a second, small energy barrier. All species in this process are singlets. The mechanism of such cycloadditions has long been the subject of controversy (see, for example, ref 56) because a definitive choice between the two main mechanisms could not be made. We will not review the extensive experimental/ theoretical work on this topic but wish to note that, given the array of possible 1,3- and 1,2-dipoles, any of the cycloaddition processes discussed above may happen or compete with each other depending on the reaction partners.

The dimerization of nitrile oxides is a special type of [3 + 2] dipolar cycloaddition, where both the 1,3- and the 1,2-dipoles are nitrile oxides. To study the dimerization of **1**, we have chosen the B3-LYP/6-31G** method, which proved capable of describing the structure of both the dimer and monomer of **1**, because it incorporates some electron correlation and is computationally feasible given resource limitations. The calculated results are summarized in Figure 6, where the 3D potential

energy surface has been obtained by first placing the two monomers apart (C−C distance, 4.0 Å), point (**1** + **1**), and then gradually decreasing this distance in defined increments while keeping the NCCN dihedral angle fixed and relaxing all other bond lengths and angles at each point of the surface. More than 120 points on the surface were obtained, including minima, transition states, and saddle points, identified by the values of the Hessian. From these B3-LYP calculations, the dimerization (Figure 6) can be characterized as a typical Firestone-type cycloaddition: a two-step mechanism, in which only one σ bond, the C−C bond, forms in the first step. The first step proceeds via a transition state (TS1) where the two dipoles are in an extended conformation (NCCN dihedral angle, 180°), leading to an energy minimum (IM) which may be identified as the Firestone intermediate. In the second step the extended intermediate, IM, closes with rotation around the established C−C single bond to the final five-membered furoxan ring **2** after passing over a second transition state (TS2) with an energy barrier of 3.0 kcal/mol. Since TS2 is 7.8 kcal/mol below TS1 and the barrier at TS1 compared to the energy of two monomers is 4.3 kcal/mol, the first step is rate determining, in agreement with Firestone's mechanism. The dimerization barrier of 4.3 kcal/mol is quite low, the calculation clearly predicting that dimerization of **1** must be spontaneous and rapid at room temperature, in agreement with the experimental findings. The potential is quite flat around the TS1 transition state; at TS1 the two CNO groups are in an extended configuration (NCCN dihedral angle is 180°), and with a decrease in the NCCN dihedral angle, the calculated barrier to dimerization increases to 9.8 kcal/mol at a NCCN dihedral angle of 0° (SP2, second-order saddle point), which is still fairly low and could be surmounted at room temperature. We have also searched for the "concerted transition state", but to no avail. SP2 could have been the wanted "concerted transition state", but it is not since the N−O distance is far too long (3.562 Å). The 1,2-dinitroso-1,2-dichloroethylene species, often postulated as an intermediate in such reactions,[57] does not appear on this surface and is not an intermediate in the lowest energy dimerization process.

Conclusion

The ClCNO molecule has been identified in the gas phase by its infrared and HeI photoelectron spectra, following thermolysis of $Cl_2C{=}NOH$(g). The structure, unobtainable from low-resolution IR, has been calculated with medium-scale ab initio calculations. Oscillations are observed in the MP*n* series, and the effects of triples is pronounced, but the conclusion is that ClCNO must be a linear or quasi-linear species with a very low barrier to linearity. The ring dimer of ClCNO has been investigated in the gas phase by HeI photoelectron, infrared, and photoionization mass spectra. The data complement that observed for other furoxans, with calculations employing DFT assisting with the spectroscopic assignments. The dimerization mechanism has been investigated with DFT, the results suggesting a low-energy process involving a two-step mechanism.

Acknowledgment. We thank the Hungarian Scientific Research Fund (OTKA Grant F022031) and the Natural Sciences and Engineering Research Council of Canada (NSERC) for research and equipment grants in support of this work. T.P. thanks NSERC for the award of a NATO Science Fellowship.

References and Notes

(1) Wieland, H. *Ber. Dtsch. Chem. Ges.* **1909**, *42*, 4192.
(2) Kekulé, A. *Justus Liebigs Ann. Chem.* **1857**, *101*, 200.
(3) Maier, G.; Teles, J. H. *Angew. Chem., Int. Ed. Engl.* **1987**, *26*, 155.
(4) Torssell, K. B. G. *Nitrile Oxides, Nitrones, and Nitronates in Organic Synthesis*; Feuer, H., Ed., Organic Nitro Chemistry Series; VCH Publishers Inc.: New York, 1988.
(5) Baldwin, J. E.; Hoskins, C.; Kruse, L. *J. Chem. Soc., Chem. Commun.* **1976**, 795. Wade, P. A.; Pillay, M. K.; Singh, S. M. *Tetrahedron Lett.* **1982**, *23*, 4563. Chiarino, D.; Napoletano, M.; Sala, A. *Synth. Commun.* **1988**, *18*, 1171.
(6) Glidewell, C.; Holden, H. D. *J. Mol. Struct.* **1982**, *89*, 325.
(7) Poppinger, D.; Radom, L. *J. Am. Chem. Soc.* **1978**, *100*, 3674.
(8) Pasinszki, T.; Westwood, N. P. C. *J. Phys. Chem.* **1995**, *99*, 6401.
(9) Pasinszki, T.; Westwood, N. P. C. *J. Am. Chem. Soc*. **1995**, *117*, 8425.
(10) Teles, J. H.; Maier, G.; Hess, B. A., Jr.; Schaad, L. J.; Winnewisser, M.; Winnewisser, B. P. *Chem. Ber*. **1989**, *122*, 753.
(11) Nguyen, M. T.; Pierloot, K.; Vanquickenborn, L. G. *Chem. Phys. Lett.* **1991**, *181*, 83.
(12) Rendell, A. P.; Lee, T. J.; Lindh, R. *Chem. Phys. Lett.* **1992**, *194*, 84.
(13) Pinnavaia, N.; Bramley, M. J.; Su, M.-D.; Green, W. H.; Handy, N. C. *Mol. Phys.* **1993**, *78*, 319.
(14) Koput, J.; Winnewisser, B. P.; Winnewisser, M. *Chem. Phys. Lett.* **1996**, *255*, 357.
(15) Handy, N. C.; Murray, C. W.; Amos, R. D. *Philos. Mag*. **1994**, *69*, 755.
(16) Pasinszki, T.; Westwood, N. P. C. *J. Chem. Soc., Chem. Commun.* **1995**, 1901. Pasinszki, T.; Westwood, N. P. C. *J. Phys. Chem.* **1996**, *100*, 16856.
(17) Pasinszki, T.; Westwood, N. P. C. Manuscript in preparation.
(18) Ungnade, H. E.; Kissinger, L. W. *Tetrahedron* **1963**, *19* (Suppl. 1), 143.
(19) Hackmann, J. T.; Knipers, J. Ger. Offen. 2,135,920, 1972.
(20) Ungnade, H. E.; Loughran, E. D. *J. Heterocyclic Chem.* **1964**, *1*, 61.
(21) Kamienski, B.; Schilf, W.; Sitkowski, J.; Stefaniak, L.; Webb, G. A. *J. Crystallogr. Spectrosc. Res.* **1989**, *19*, 1003.
(22) Witanowski, M.; Stefaniak, L.; Grabowska, A.; Webb, G. A. *Spectrochim. Acta* **1978**, *34A*, 877.
(23) Všetečka, V.; Fruttero, R.; Gasco, A.; Exner, O. *J. Mol. Struct.* **1994**, *324*, 277.
(24) Pasinszki, T.; Ferguson, G.; Westwood, N. P. C. Manuscript in preparation.
(25) Pasinszki, T.; Ferguson, G.; Westwood, N. P. C. *J. Chem. Soc., Perkin Trans 2* **1996**, 179.
(26) Gryszkiewicz-Trochimowski, E.; Dymowski, K.; Schmidt, E. *Bull. Soc. Chim. Fr.* **1948**, 597.
(27) Frost, D. C.; Lee, S. T.; McDowell, C. A.; Westwood, N. P. C. *J. Electron Spectrosc. Relat. Phenom.* **1977**, *12*, 95.
(28) Koopmans, T. *Physica* **1933**, *1*, 104.
(29) Niessen, W. von; Schirmer, J.; Cederbaum, L. S. *Comput. Phys. Rep.* **1984**, *1*, 57.
(30) Frisch, M. J.; Trucks, G. W.; Head-Gordon, M.; Gill, P. M. W.; Wong, M. W.; Foresman, J. B.; Johnson, B. G.; Schlegel, H. B.; Robb, M. A.; Replogle, E. S.; Gomperts, R.; Andres, J. L.; Raghavachari, K.; Binkley, J. S.; Gonzalez, C.; Martin, R. L.; Fox, D. J.; Defrees, D. J.; Baker, J.; Stewart, J. J. P.; Pople, J. A. *Gaussian 92, Revision E.1*; Gaussian, Inc.: Pittsburgh, PA, 1992.
(31) Frisch, M. J.; Trucks, G. W.; Schlegel, H. B.; Gill, P. M. W.; Johnson, B. G.; Robb, M. A.; Cheeseman, J. R.; Keith, T. A.; Petersson, G. A.; Montgomery, J. A.; Raghavachari, K.; Al-Laham, M. A.; Zakrzewski, V. G.; Ortiz, J. V.; Foresman, J. B.; Cioslowski, J.; Stefanov, B. B.; Nanayakkara, A.; Challacombe, M.; Peng, C. Y.; Ayala, P. Y.; Chen, W.; Wong, M. W.; Andres, J. L.; Replogle, E. S.; Gomperts, R.; Martin, R. L.; Fox, D. J.; Binkley, J. S.; Defrees, D. J.; Baker, J.; Stewart, J. P.; Head-Gordon, M.; Gonzalez, C.; Pople, J. A.: *Gaussian 94, Revision A.1*; Gaussian, Inc.: Pittsburgh, PA, 1995.
(32) Pasinszki, T.; Westwood, N. P. C. *J. Mol. Struct*. **1997**, *408/409*, 161.
(33) Pasinszki, T.; Westwood, N. P. C. *J. Chem. Soc., Faraday Trans*. **1997**, *93*, 43.
(34) Freitag, W. O.; Nixon, E. R. *J. Chem. Phys*. **1956**, *24*, 109.
(35) Appel, R.; Siray, M. *Angew. Chem., Int. Ed. Engl.* **1983**, *22*, 785.
(36) Klapstein, D.; Nemes, L.; Pasinszki, T.; Westwood, N. P. C. Manuscript in preparation.
(37) Zhang, K.; Bernath, P. F.; Pasinszki, T.; Westwood, N. P. C. Manuscript in preparation.
(38) Guo, B.; Pasinszki, T.; Westwood, N. P. C.; Zhang, K.; Bernath, P. F. *J. Chem. Phys.* **1996**, *105*, 4457.
(39) Eland, J. H. D. *Philos. Trans. R. Soc. London A* **1970**, *268*, 87.
(40) Heilbronner, E.; Hornung, V.; Muszkat, K. A. *Helv. Chim. Acta* **1970**, *53*, 347. Lake, R. F.; Thompson, H. *Proc. R. Soc. Lond*. A. **1970**, *317*, 187.

(41) Kimura, K.; Katsumata, S.; Achiba, Y.; Yamazaki, T.; Iwata, S. *Handbook of HeI Photoelectron Spectra of Fundamental Organic Molecules*; Japan Scientific Societies Press: Tokyo, 1981.

(42) Bunker, P. R.; Landsberg, B. M.; Winnewisser, B. P. *J. Mol. Spectrosc.* **1979**, *74*, 9. Jensen, P. *J. Mol. Spectrosc.* **1983**, *101*, 422.

(43) Brupbacher, Th,; Bohn, R. K.; Jäger, W.; Gerry, M. C. L.; Pasinszki, T.; Westwood, N. P. C. *J. Mol. Spectrosc.* **1997**, *181*, 316.

(44) Guo, B.; Pasinszki, T.; Westwood, N. P. C.; Bernath, P. F. *J. Chem. Phys.* **1995**, *103*, 3335.

(45) Pople, J. A.; Head-Gordon, M.; Raghavachari, K. *Int. J. Quantum Chem., Quantum Chem. Symp.* **1988**, *22*, 377. Kraka, E.; Gauss, J.; Cremer, D. *J. Mol. Struct. (THEOCHEM)* **1991**, *80*, 95.

(46) He, Z.; Cremer, D. *Int. J. Quantum Chem., Quantum Chem. Symp.* **1991**, *25*, 43. He, Z.; Cremer, D. *Theor. Chim. Acta* **1993**, *85*, 305.

(47) Lichau, H.: Winnewisser, B. P.; Winnewisser, M. Private communication.

(48) Weinhold, F.; Carpenter, J. E. *The Structure of Small Molecules and Ions*; Plenum: New York, 1988.

(49) Boyer, N. E.; Czerniak, G. M.; Gutowsky, H. S.; Snyder, H. R. *J. Am. Chem. Soc.* **1955**, *77*, 4238. Boyer, J. H.; Toggweiler, U.; Stoner, G. A. *J. Am. Chem. Soc.* **1957**, *79*, 1748. Kropf, H.; Lambeck, R. *Liebigs Ann. Chem.* **1966**, *700*, 18.

(50) Palmer, M. H.; Findlay, R. H.; Egdell, R. G. *J. Mol. Struct.* **1977**, *40*, 191.

(51) Maier, J. P.; Muller, J.-F. *J. Chem. Soc., Faraday Trans 2*, **1974**, *70*, 1991.

(52) Veszprémi, T.; Nyulászi, L.; Zsombok, Gy. *J. Electron Spectrosc. Relat. Phenom.* **1988**, *46*, 269. Veszprémi, T.; Nyulászi, L.; Zsombok, Gy.; Réffy, J.; Cvitaš, T.; Kovač, B.; Klasinc, L. *J. Mol. Struct (THEOCHEM)* **1989**, *202*, 227.

(53) Huisgen, R. *Angew. Chem., Int. Ed. Engl.* **1963**, *2*, 565; *J. Org. Chem.* **1968**, *33*, 2291; **1976**, *41*, 403.

(54) Huisgen, R. In *1,3-Dipolar Cycloaddition Chemistry;* Padwa, A., Ed.; Wiley-Interscience: New York, 1984; Vol. 1.

(55) Firestone, R. A. *J. Org. Chem.* **1968**, *33*, 2285; **1972**, *37*, 2181; *J. Chem. Soc. A* **1970**, 1570; *Tetrahedron* **1977**, *33*, 3009.

(56) Houk, K. N.; Yamaguchi, K. In *1,3-Dipolar Cycloaddition Chemistry*; Padwa, A., Ed.; Wiley-Interscience: New York, 1984; Vol. 2.

(57) Sedano, E.; Sarasola, C.; Ugalde, J. M.; Irazabalbeitia, I. X.; Guerrero, A. G. *J. Phys. Chem.* **1988**, *92*, 5094; Sedano, E.; Sarasola, C.; Ugalde, J. M. *Tetrahedron.* **1989**, *45*, 6537; Seminario, J. M.; Concha, M. C.; Politzer, P.; *J. Comput. Chem.* **1992**, *13*, 177; Friedrichsen, W. *J. Mol. Struct.* **1995**, *342*, 23; Klenke, B.; Friedrichsen, W. *Tetrahedron* **1996**, *52*, 743.